Numerical investigation on spontaneous droplet/bubble migration under thermal radiation

Bo Zhang[a], Dong Liu[a], Yongpan Cheng[a,b,c,*], Jinliang Xu[a,b,**], Yi Sui[c]

[a] Key Laboratory of Condition Monitoring and Control for Power Plant Equipment of Ministry of Education, North China Electric Power University, Beijing 102206, China
[b] Beijing Key Laboratory of Multiphase Flow and Heat Transfer for Low Grade Energy, North China Electric Power University, Beijing 102206, China
[c] School of Engineering and Materials Science, Queen Mary University of London, Mile End Road, London, E1 4NS, United Kingdom

ARTICLE INFO

ABSTRACT

The spontaneous migration of droplet/bubble has widely application in manipulating droplet/bubble in microgravity. In this study the droplet/bubble migration due to thermal capillary force under uniform incoming thermal radiation is numerically investigated. The numerical model is based on the transient two-dimensional axisymmetric model with a level set method. After validation with the analytical solution under low Reynolds numbers and Marangoni numbers, the study is extended to the droplet/bubble migration under high Reynolds numbers and Marangoni numbers. The ratios are defined as the values in the outer continuous phase over those in the inner discrete phase. The ratios of dynamic viscosity, thermal conductivity, density and specific heat on the migration velocities of droplet/bubble are investigated under all Reynolds numbers. It is found that the droplet/bubble can migrate spontaneously under thermal radiation due to thermal capillary effect, the driving force is from the induced pressure drop in the middle region of droplet/bubble. Under low Reynolds numbers the migration velocities depend only on the ratios of dynamic viscosity and thermal conductivity, while under high Reynolds numbers they also depend on the ratios of density and specific heat. Under all Reynolds numbers the migration velocities are the lowest when the dynamic viscosity or thermal conductivity in the continuous phase is equal to that in the discrete droplet/bubble phase. With the increasing difference between the continuous phase and discrete phase, the migration velocities are increased. This study might be helpful for manipulating droplet/bubble through thermal capillary force with incoming thermal radiation.

1. Introduction

The thermal capillary effect is caused by the uneven surface tension distribution due to temperature difference along the interface between two immiscible fluids. The thermal capillary force can drive the bubble or droplet to migrate, which have been widely studied by the researchers. Under gravity the thermocapillary force may be suppressed by the buoyant or gravitational force, while under microgravity the thermal capillary force may become dominant and it can be adopted to manipulate the bubble/droplet dynamics, such as in recycling water and oxygen in the long duration space excursions [1].

Young et al. [2] first studied the thermal capillary migration of bubbles under temperature gradient when the momentum and energy transport are both negligible. The analytical solution on migration velocity was provided under thermal capillary and gravitational effects. This solution was proved by Balasubramaniam and Chai [3] to be still

applicable to any Reynolds number only if $Ma < < 1$. Crespo et al. [4] analyzed the thermal capillary migration of bubbles at large Reynolds number and arbitrary Marangoni numbers. Crespo and Jimenez-Fernandez [5] carried out analysis and got the expression of bubble migration velocity in the limit of both $Re > > 1$ and $Ma > > 1$.

Besides the theoretical analysis, experimental work has also been carried out to study the droplet/bubble migration under microgravity. Thompson et al. [6] investigated migration of the nitrogen bubbles under a temperature gradient in various liquids in the drop tower, the results are consistent with predictions from linear theory for negligible Reynolds and Marangoni numbers. Balasumbramaniam et al. [1] studied the motion of isolated droplets and bubbles in a silicone oil under an applied temperature gradient at moderate Marangoni numbers in a reduced gravity. They found that the scaled velocity decreases with increasing Marangoni number, and it approaches the theoretical asymptote in the limit of large Marangoni numbers. Xie et al. [7]

Nomenclature

Ca	Capillary number		u_0	Reference velocity
C_p	Dimensional specific heat		u_∞	Bulk velocity of droplet or bubble
C_p^*	Non-dimensional specific heat		u_m	Dimensional migration velocity
dx	Grid size		u_m^*	Non-dimensional migration velocity
f	Surface tension		v^*	Non-dimensional velocity
H	Heaviside function		x^*, y^*	Non-dimensional coordinates
Ma	Marangoni number		α	Absorptivity of the droplet/bubble surface
$\vec{n}$	Normal vector		θ	Tangential angle
Nu	Nusselt number		δ	Dirac delta function
p	Dimensional pressure		ε	Non-dimensional thickness of interface
p^*	Non-dimensional pressure		ϕ^*	Non-dimensional function
Pr	Prandtl number		κ	Dimensional curvature
q_r	Thermal radiation flux		κ^*	Non-dimensional curvature
r_0	Droplet/Bubble radius		λ	Dimensional thermal conductivity
Re	Reynolds number		λ^*	Non-dimensional thermal conductivity
R_v	Ratio of the dynamic viscosity		λ_l	Thermal conductivity of liquid
R_c	Ratio of the thermal conductivity		μ	Dimensional dynamic viscosity
R_d	Ratio of the density		μ^*	Non-dimensional dynamic viscosity
R_{C_p}	Ratio of the specific heat		μ_l	Dynamic viscosity of liquid
T	Dimensional temperature		ρ	Dimensional density
T^*	Non-dimensional temperature		ρ^*	Non-dimensional density
T_0	Reference temperature		ρ_l	Density of liquid
T_{max}	Maximum temperature		σ	Surface tension
t	Dimensional time		σ_0	Surface tension at ambient temperature
t^*	Non-dimensional time		σ_T	Variation coefficient of surface tension over temperature
u	Dimensional velocity		g	Gas
u^*	Non-dimensional velocity		l	Liquid
			s	Surface

studied the motion of isolated drops of Fluorinert liquid in the silicone oil, and found that scaled drop migration velocity decreases with the increasing Marangoni number up to 5500. The experimental studies on the microgravity were carried out through either drop tower or outer space, which brings great difficulties due to the short experimental time or its cost, especially for experiment at large Reynolds or Marangoni numbers. On the contrary, the numerical simulation provides a feasible and efficient way to carry out the studies.

Szymczyk et al. [8] early simulated the bubble migration with non-zero Reynolds number and large Marangoni number with a two-dimensional model. Through simulation Balasubramaniam and Lavery [9] found that the scaled velocities of bubbles have only modest variation for different Reynolds numbers, while the Marangoni number have larger effect on the migration velocity. Ma et al. [10] found that at fairly large Marangoni numbers, the migration velocity is independent of Marangani number. Haj-Hariri et al. [11] simulated an isolated drop motion by using three-dimensional model, and found that the inertial effect on the mobility of viscous droplets is weaker than that of gas bubbles. Yin et al. [12] studied the thermal capillary migration of non-deformable drops under different ratios of drop densities and specific heats over those of continuous phases, and discussed the influence of initial conditions on the thermal capillary migrations. They [13] also extended their studies to the thermal capillary migration with large Marangoni numbers. They found that there is nontrivial difference among the migration velocities in theoretical analysis, numerical simulations and space experiments, this is caused by the different migrating distances to reach steady stages in different investigations. Wu [14] investigated the terminal thermal capillary migration of a droplet with slight deformation, and revealed that the terminal thermal capillary migration is unsteady at small Reynolds numbers and large Marangoni numbers.

From the review above, it can be seen that all the studies on droplet/bubble migration under thermal capillary effect are caused by the temperature gradient, there are seldom studies on the thermal capillary

migration under heat flux. The droplet/bubble thermal capillary migration under radiation heat flux is often encountered in outer space. Oliver and DeWitt derived [15] the analytical solution for thermal capillary migration of droplet with negligible Reynolds and Marangoni numbers under constant radiation heat flux under microgravity. The purpose of our paper is to extend their study to higher Reynolds numbers and Marangoni numbers, the effect of physical properties on droplet/bubble against continuous phases on the migration velocity will also be revealed, this may be of great significance for thermal radiation-induced thermal capillary migration under microgravity.

In the following sections, the physical model and mathematical formulation will be introduced first, followed by the validation of current model with analytical solution under low Reynolds numbers, then it will be extended to high Reynolds numbers through numerical simulation. The effect of ratios of dynamic viscosity, thermal conductivity, density and specific heat on the migration velocities and Nusselt numbers are investigated. Finally, some conclusions will be drawn for spontaneous migration of droplet/bubble with uniform incoming thermal radiation.

2. Physical model and mathematical formulation

Fig. 1 is the schematic diagram of the migration of droplet/bubble under the uniform radiation heat flux. It is assumed that the droplet/bubble is a gray body, and the heat absorption only occurs at the interfaces. The heat absorption rate of droplet/bubble varies with the cosine of the tangential angle with the incoming thermal radiation. Due to the difference of temperature difference at the interfaces, the thermal capillary force will be generated and drives the droplet/bubble towards the direction of incoming thermal radiation. When the thermal capillary force is in balance with the pressure drop, viscous force and inertial force, the migration of droplet/bubble will reach a steady stage.

The governing equations for the migration of droplet/bubble under thermal radiation are as follows:
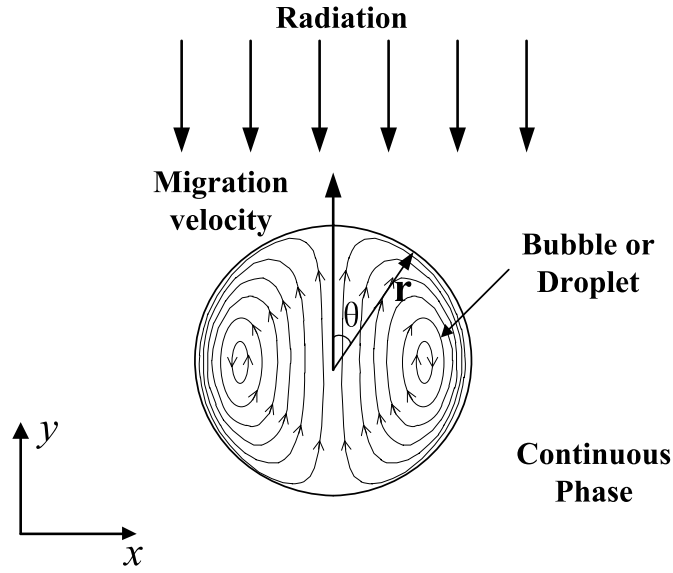
Fig. 1. Schematic diagram of droplet/bubble migration under thermal capillary force due to uniform incoming thermal radiation.

The continuity equation

$$\nabla \cdot \vec{u} = 0 \tag{1}$$

The momentum equation

$$\rho \frac{\partial \vec{u}}{\partial t} + \rho \vec{u} \cdot \nabla \vec{u} = -\nabla p + \nabla \cdot [\mu(\nabla \vec{u} + \nabla \vec{u}^T)] + \vec{f_s} \tag{2}$$

The energy equation

$$\rho C_p \frac{\partial T}{\partial t} + \rho C_p \vec{u} \cdot \nabla T = \nabla \cdot (\lambda \nabla T) + q_r \cos \theta \; \delta(\phi) \tag{3}$$

In the momentum equation (2), $\vec{f_s}$ is the surface tension at the gas-liquid interface which includes two parts, one is the force in the normal direction of the interface, the other is the thermal capillary force in the tangential direction along the interface. It is assumed that the surface tension is the function of temperature as $\sigma(T) = \sigma_0 - \sigma_T(T - T_\infty)$. Thus the surface tension

$$\vec{f_s} = \kappa \sigma(T) \delta(\phi) \vec{n} - \sigma_T \nabla_s T \delta(\phi) \tag{4}$$

In the energy equation (3), it is assumed that only the interface of upper part of droplet/bubble can absorb the thermal radiation, and it varies with the cosine of the tangential angle with the incoming thermal radiation. The interface of lower part of droplet/bubble will not absorb the thermal radiation, hence the tangential angle is in the following range, $0 \le \theta \le 90^\circ$. $\delta(\phi)$ is the Dirac delta function, it can distribute the surface tension and thermal radiation into the interface.

The characteristic velocity is defined based on the thermal capillary induced velocity under constant thermal radiation

$$u_0 = -\frac{\sigma_T \alpha q_r r_0}{\lambda_l \mu_l} \tag{5}$$

The characteristic temperature difference is defined based on the thermal radiation-induced temperature difference

$$\Delta T_0 = \frac{q_r r_0}{\lambda_l} \tag{6}$$

The characteristic length is the droplet/bubble radius r_0, thus the non-dimensional governing equations are as follows:

The continuity equation

$$\nabla \cdot \vec{u}^* = 0 \tag{7}$$

The momentum equation

$$\frac{\partial \vec{u}^*}{\partial t^*} + \vec{u}^* \cdot \nabla \vec{u}^* = -\frac{1}{\rho^*} \nabla p^* + \frac{1}{\rho^* \mathrm{Re}} \nabla \cdot [\mu^*(\nabla \vec{u}^* + \nabla \vec{u}^{*T})]$$
$$+ \frac{1 - Ma \cdot T^*}{\rho^* \mathrm{Re} \cdot Ca} \kappa^* \vec{n} \delta(\phi^*) - \frac{Ma}{\rho^* \mathrm{Re} \cdot Ca} \nabla_s T^* \delta(\phi^*) \tag{8}$$

The energy equation

$$\frac{\partial T^*}{\partial t^*} + \vec{u}^* \cdot \nabla T^* = \frac{1}{\rho^* C_p^* \mathrm{Re} \cdot Pr} \nabla \cdot (\lambda^* \nabla T^*) + \frac{\delta(\phi^*) \cos \theta}{\rho^* C_p^* \mathrm{Re} \cdot Pr} \tag{9}$$

It is noted that the variables with asteroid are all non-dimensional. The non-dimensional physical properties are defined based on the values of liquid as follows:

For droplet migration

$$\rho^* = H + (1 - H)R_d \tag{10a}$$

$$\mu^* = H + (1 - H)R_v \tag{10b}$$

$$\lambda^* = H + (1 - H)R_c \tag{10c}$$

$$C_p^* = H + (1 - H)R_{C_p} \tag{10d}$$

For bubble migration

$$\rho^* = (1 - H) + H/R_d \tag{11a}$$

$$\mu^* = (1 - H) + H/R_v \tag{11b}$$

$$\lambda^* = (1 - H) + H/R_c \tag{11c}$$

$$C_p^* = (1 - H) + H/R_{C_p} \tag{11d}$$

The ratios of density R_d, dynamic viscosity R_v, thermal conductivity R_c and specific heat R_{C_p} are defined with the values of the outer continuous phase over the inner discrete phase, hence the ratios are less than 1 for droplet migration and are larger than 1 for the bubble migration.

H is the Heaviside function

$$H_\varepsilon(\phi^*) = \begin{cases} 0 & \phi^* < -1.5dx \\ \frac{1}{2}\left[1 + \frac{\phi^*}{\varepsilon} + \frac{1}{\pi}\sin\left(\frac{\pi\phi^*}{\varepsilon}\right)\right] & |\phi^*| \le 1.5dx \\ 1 & \phi^* > 1.5dx \end{cases} \tag{12}$$

The level set function is solved from the level set convection equation to track the interface

$$\frac{\partial \phi^*}{\partial t^*} + \vec{u}^* \cdot \nabla \phi^* = 0 \tag{13}$$

To ensure that ϕ^* is the distance from the interface, the re-initialization is adopted in each step.

Due to the symmetry of droplet/bubble in y direction, the axisymmetric model with a level set method is adopted to investigate the droplet/bubble migration. The governing equations are discretized on a marker-and-cell (MAC) mesh, and the velocities are defined at cell faces, the scalar variables are defined at the cell centers. The standard projection method is adopted to solve the continuity equation and momentum equation. The temporal advection term is discretized with Adams-Bashforth scheme and the temporal diffusion term is discretized with Crank-Nicolson scheme. For the level set advection equation and energy equation, the advection term is spatially discretized with a fifth-order Weighted Essentially Non-Oscillatory (WENO) scheme. The diffusion terms are spatially discretized with the second-order central difference scheme.

Due to the symmetry of droplet/bubble in y direction, only the right half of droplet/bubble is simulated. After sensitivity study, the grid size is taken as 201×601, the computational domain is taken as 4×12, and the time step is taken as 1×10^{-4}. The convergence criterion in each time step is that the residues of both continuity and energy equations are below 1×10^{-3}. The default parameter settings are $\mathrm{Re} = 1$, $Ma = 0.1$ and $R_v = R_c = R_d = R_{C_p} = 1$.

The boundary conditions are as follows:

Left boundary ($x^* = 0$)
　Symmetric: $u^* = 0$, $\frac{\partial v^*}{\partial x^*} = 0$, $\frac{\partial T^*}{\partial x^*} = 0$
Right boundary ($x^* = 4$)
　Free boundary: $v^* = 0$, $\frac{\partial u^*}{\partial x^*} = 0$, $\frac{\partial T^*}{\partial x^*} = 0$
Lower boundary ($y^* = 0$)
　Free boundary: $u^* = 0$, $\frac{\partial v^*}{\partial y^*} = 0$, $\frac{\partial T^*}{\partial y^*} = 0$
Upper boundary ($y^* = 12$)
　Free boundary: $u^* = 0$, $\frac{\partial v^*}{\partial y^*} = 0$, $\frac{\partial T^*}{\partial y^*} = 0$

In order to evaluate the relative importance of different forces, the following non-dimensional numbers are defined based on the values of liquid.

$$Re = \frac{\rho_l u_0 r_0}{\mu_l} \tag{14a}$$

Capillary number

$$Ca = \frac{\mu_l u_0}{\sigma_0} \tag{14b}$$

Effective Marangoni number

$$Ma = \frac{\sigma_T q_r r_0}{\lambda_l \sigma_0} \tag{14c}$$

The Nusselt number

$$Nu = \frac{q_r r_0}{\lambda_l T_{\max}} \tag{14d}$$

3. Results and discussion

3.1. Numerical validation

In order to test the validation of current numerical model, the numerical results are compared with the analytical solution. For the stokes flow when the Re and Ma numbers are very low (Re < 1 and Ma < 1), Oliver and DeWitt [15] provided the analytical solution of droplet migration velocity under parallel incoming thermal radiation as

$$u_m = -\frac{\sigma_T \alpha q_r r_0}{3\lambda_l \mu_l (2 + 3R_v)(2 + R_c)} \tag{15}$$

After normalization with characteristic velocity in Eq. (5), the normalized migration velocity

$$u_m^* = \frac{1}{3(2 + 3R_v)(2 + R_c)} \tag{16}$$

It can be seen that the normalized migration velocity depends only on the ratio of viscosity and thermal conductivity. In Fig. 2 the numerical results are compared with the analytical solutions under different ratios of dynamic viscosity and thermal conductivity. It can be found that the numerical results agree quite well with the analytical solution. The numerical results are also compared with the experiments for thermal capillary-induced droplet migration under temperature gradient with low Reynolds number and Marangoni number [16], the predicted migration velocity 0.22 μm/s is quite close to the experimental value 0.20 ± 0.03μm/s, this also proves that our model is accurate and robust.

The migration velocity of droplet/bubble is determined by the inertial force, pressure drop, viscous force and the thermal capillary force, which are provided as follows:

$$\overrightarrow{F}_{net}^* = \rho^* \frac{d\overrightarrow{u_m}^*}{dt^*} = \int_\Omega \rho^* \overrightarrow{u}^* \cdot \nabla \overrightarrow{u}^* dv + \int_S p^* d\overrightarrow{s} + \int_S \mu^* (\nabla \overrightarrow{u}^* + \nabla \overrightarrow{u}^{*T}) \cdot d\overrightarrow{s}$$
$$+ \int_S \left(\frac{1 - MaT^*}{Re\,Ca} \kappa^* \overrightarrow{n} - \frac{Ma}{Re\,Ca} \nabla_s T^* \right) \cdot d\overrightarrow{s} \tag{17}$$

Here Ω is the droplet/bubble region, S is the gas-liquid interface. Take the default case (Re = 1, Ma = 0.1, the ratios $R_v = R_c = R_d = R_{C_p} = 1$) as example, the transient variations of individual forces are provided in Fig. 3. It can be seen that upon the absorption of thermal radiation, the thermal capillary force, inertial force, viscous force and pressure drop are generated. It is interesting to note that the pressure drop is positive while the viscous force and thermal capillary force are negative, and the inertial force is negligible due to the low Reynolds numbers. The pressure drop is the main driving force for droplet/bubble migration. In the initial stage the pressure drop and viscous force are increased dramatically, then they will approach almost constant when the droplet/bubble reaches the quasi-steady migration. Under the interaction of these forces, the resultant driving
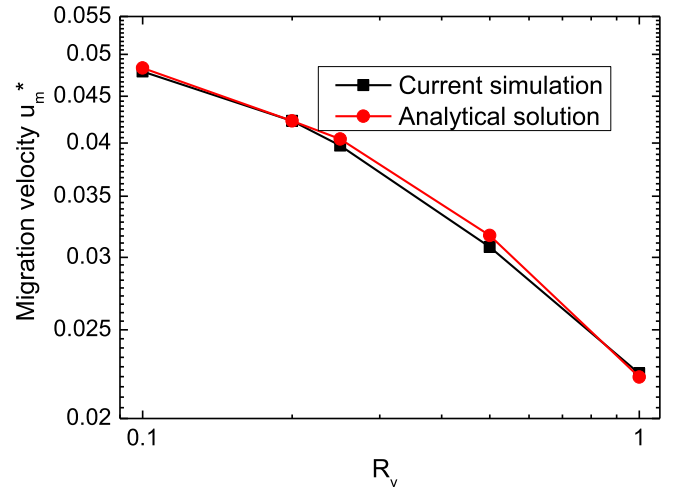
(a) Dynamic viscosity
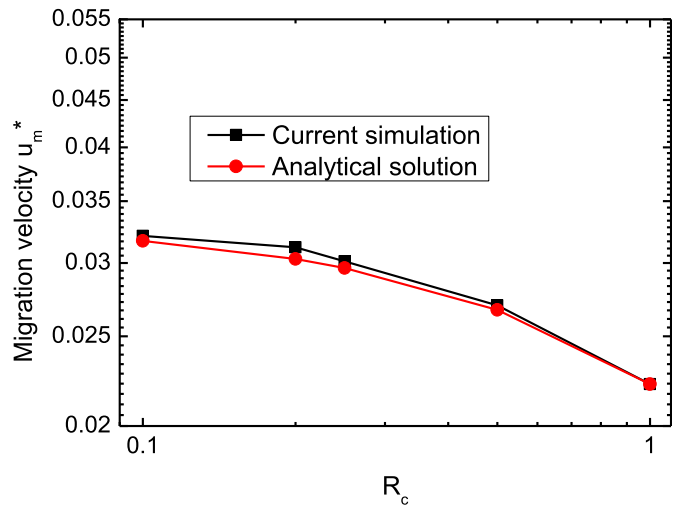
(b) Thermal conductivity

Fig. 2. Comparison of numerical results with analytical solution for droplet migration under uniform thermal radiation under different ratios of dynamic viscosity R_v and thermal conductivity R_c.
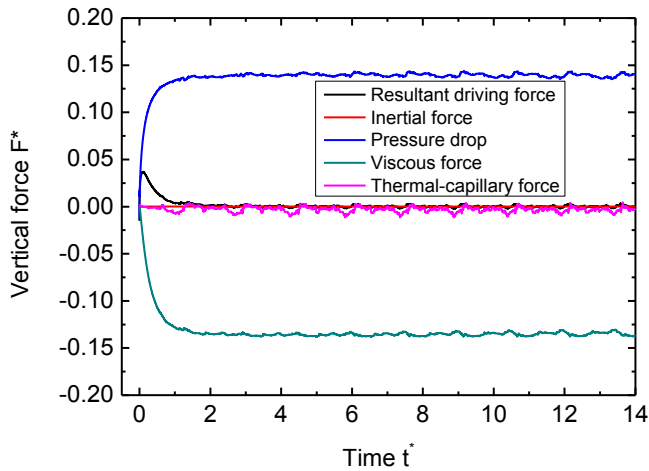
Fig. 3. Transient variation of forces on the droplet/bubble at Re = 1, Ma = 0.1 and the ratios $R_v = R_c = R_d = R_{C_p} = 1$.

force for droplet/bubble migration will increase dramatically at the initial stage, and it will reach the maximum at around t = 0.1, then it will decrease mildly until it reaches zero at quasi-steady migration state.

In Fig. 4 the upward migration velocity of droplet/bubble is shown, it can be seen that the droplet/bubble can migrate spontaneously under the thermal radiation. At the initial stage, due to the non-uniform distribution of temperature along the gas-liquid interface, temperature gradient is generated, resulting in the tangential thermal capillary force from the top to the bottom along the gas-liquid interface. The thermal capillary force will drive the fluid downward along the interface. In order to compensate the mass loss at the upper region of droplet/bubble, the liquid will flow from the lower region to the upper region, and flow downward again along the interface, as seen in Fig. 5. Therefore the pressure at the lower region is higher than that at the upper region, this pressure drop will drive the droplet/bubble to move upward. After the pressure drop is in balance with the viscous force, thermal capillary force and inertial force, the droplet/bubble will reach the quasi-steady migration stage. Due to the interaction between the flow field and temperature field, the droplet/bubble will deform slightly during the migration, hence the forces and migration velocity will fluctuate periodically, as seen in Figs. 3 and 4.

3.2. The effect of dynamic viscosity ratio on migration velocity

In Fig. 6 the effect of dynamic viscosity ratio on the migration velocity of droplet/bubble is shown under different Reynolds numbers. As the ratio is defined as the value of outer continuous phase over that of the inner discrete phase, it corresponds to the droplet migration at $R_v < 1$, and bubble migration at $R_v > 1$. It is obvious that at $R_v = 1$, the migration velocity is the minimum. In the droplet regime, with the decreasing ratio of dynamic viscosity, the viscous force along the gas-liquid interface is reduced, the tangential flow induced by thermal capillary force becomes stronger, leading to stronger upward flow in the middle region of droplet, so the resultant migration velocity is also increased. Take the case at Re = 1 as example, at the dynamic viscosity ratio $R_d = 1$, the driving pressure drop is around 0.137, corresponding to the migration velocity 0.0222, while when the ratio of dynamic viscosity is reduced to 0.1, the driving pressure drop is around 0.215, corresponding to the migration velocity 0.0458.

In the bubble regime, with the increasing ratio of dynamic viscosity the migration velocity increases rapidly first and then approaches a plateau, because the viscous force on bubble will be almost constant with further increasing dynamic viscosity in the outer continuous phase. In comparison the dynamic viscosity has more significant effect

on the bubble, because the bubble has lower inertia than the droplet and it is easily affected by the viscous force.

3.3. The effect of thermal conductivity ratio on migration velocity

In Fig. 7 the effect of thermal conductivity ratio on the migration velocity of droplet/bubble is shown under different Reynolds numbers. It is noted that the thermal conductivity ratio has more significant effect on the bubble than the droplet. In this simulation the dynamic viscosity ratio between the continuous phase and discrete phase is default 1. In the droplet regime, with the decreasing ratio of thermal conductivity the temperature distribution along the interface will become more non-uniform, leading to large thermal capillary force along the gas-liquid interface, the circulating flow inside the droplet becomes stronger. Take the case at Re = 1 as example, when the ratio is reduced from 1 to 0.1, the driving pressure drop is increased from 0.137 to 0.331, and the corresponding migration velocity is increased from 0.0222 to 0.0321.

3.4. The effect of Reynolds number on migration velocity

The migration of droplet/bubble under low Reynolds numbers and Marangoni numbers can be derived from the theoretical analysis, while at high Reynolds numbers or Marangoni numbers there is no analytical solution, hence in our study the numerical simulation will be carried out to study the migration of droplet/bubble under high Reynolds numbers or Marangoni numbers. The effect of ratios of dynamic viscosity, thermal conductivity, density and specific heat on the migration velocity is shown as below.

3.4.1. Under different ratios of dynamic viscosity

In Fig. 8 the effect of Reynolds numbers on the migration velocity is shown under different ratios of dynamic viscosity, it can be found that with the increasing Reynolds numbers, the migration velocities decrease mildly at first, then they will decrease dramatically, especially for the droplet. At low Reynolds numbers the flow around droplet/bubble is viscous flow, and heat transfer is mainly through heat conduction, the temperature gradient along the surface is quite large, leading to the high driving thermal capillary force; However, at high Reynolds number the convective heat transfer becomes significant, which is more efficient than heat conduction, thus the temperature gradient along the surface becomes low, leading to low thermal capillary force. It is also noted that the Reynolds number has more significant effect on droplet than that on bubble.
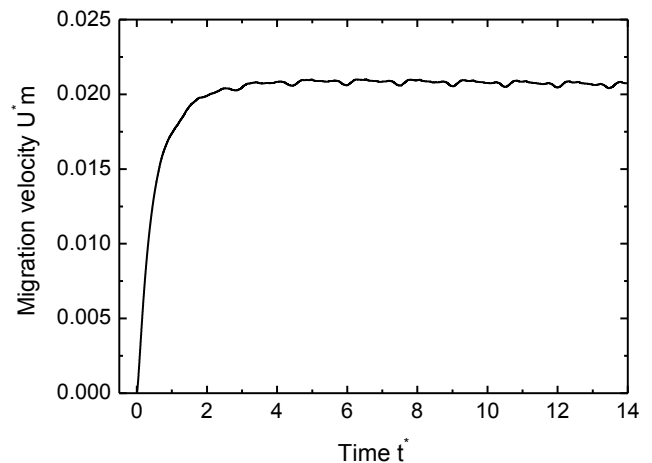

Fig. 4. Transient variation of droplet/bubble migration velocity at Re = 1, Ma = 0.1 and the ratios $R_v = R_c = R_d = R_{C_p} = 1$.
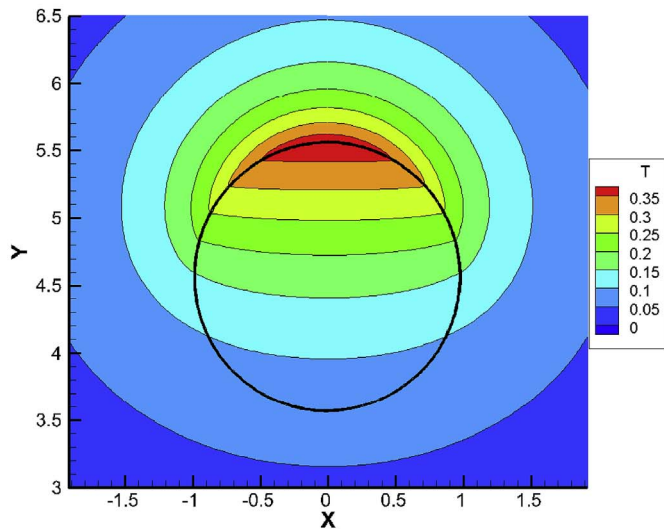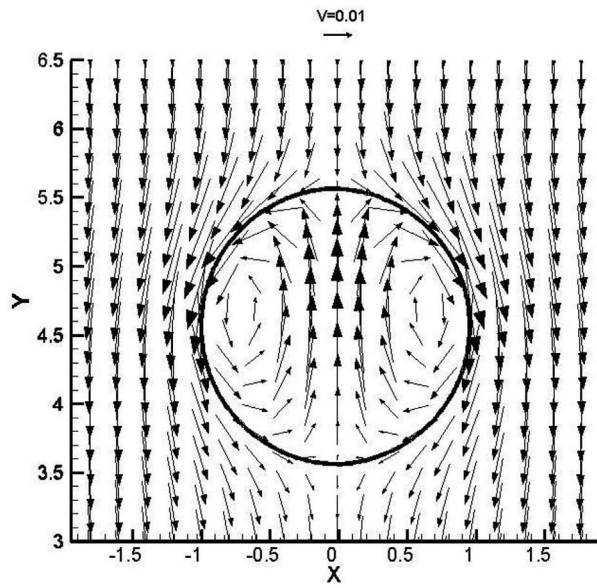
Fig. 5. Velocity and temperature fields at Re = 1, Ma = 0.1 and $R_v = R_c = R_d = R_{Cp} = 1$ at steady state.
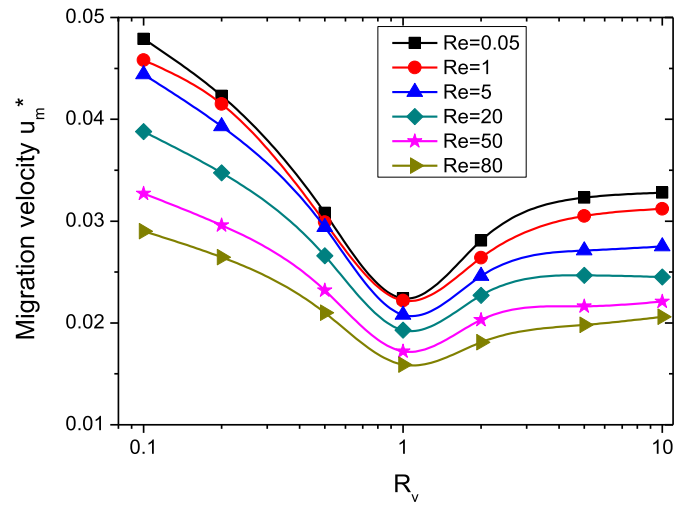

Fig. 6. Effect of dynamic viscosity ratio on the migration velocity under different Reynolds numbers.
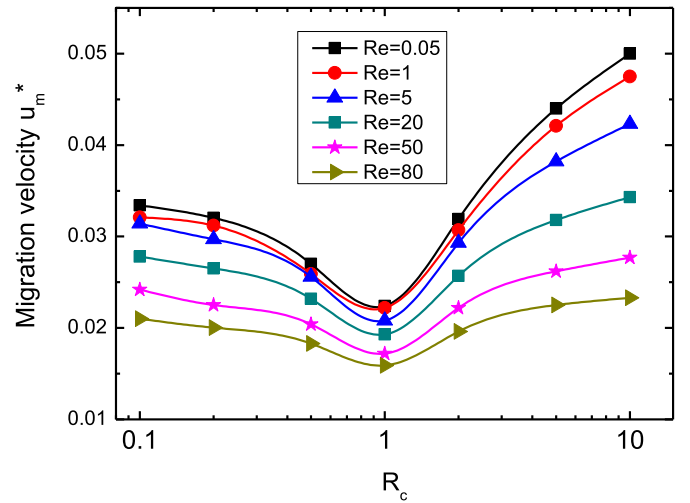

Fig. 7. Effect of thermal conductivity ratio on the migration velocity under different Reynolds numbers.
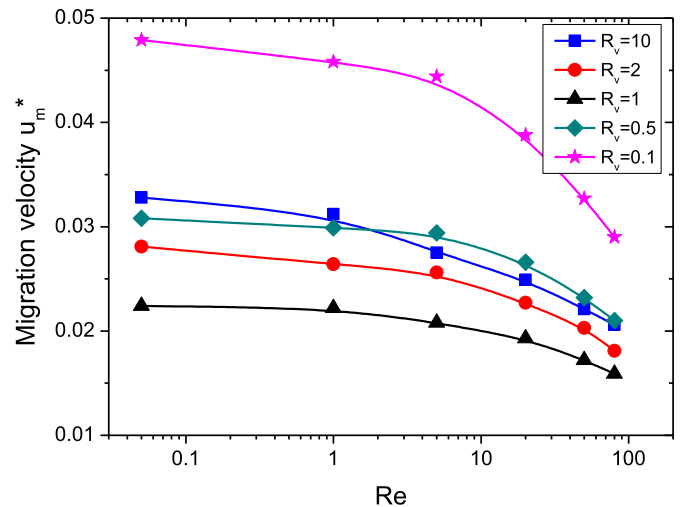

Fig. 8. Effect of Reynolds numbers on migration velocity under different ratios of dynamic viscosity.
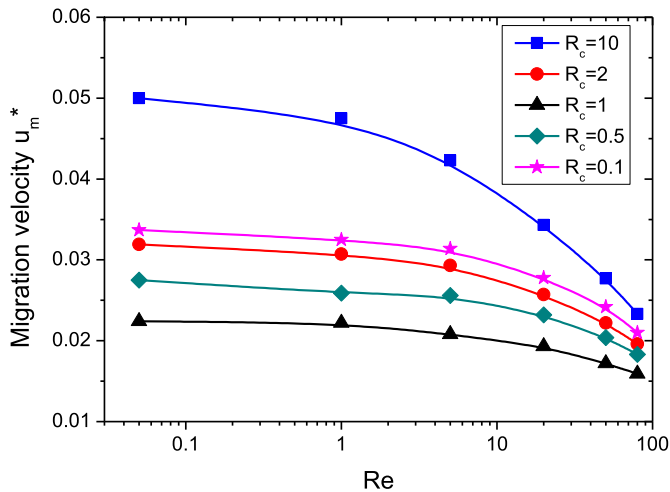
3.4.2. Under different ratios of thermal conductivity

In Fig. 9 the effect of Reynolds number on the migration velocity of droplet/bubble is shown under different ratios of thermal conductivity. It is found that with the increasing Reynolds number, the migration velocities decrease quite mildly at low Reynolds numbers, and then decrease dramatically at high Reynolds numbers. The effect of Reynolds number on the bubble is more significant than that on the droplet.

For example, when the Reynolds number is increased from 0.05 to 80, for bubble with ratio of thermal conductivity 10, the migration velocity is reduced by around 53%, while for the droplet with ratio of thermal conductivity 0.1, the migration velocity is reduced only around 37%. Consistent with the results in the previous sections, the migration velocity is the minimum when the ratio is 1. With decreasing ratio for droplet or increasing ratio for bubble, the migration velocities all increase.

3.4.3. Under different ratios of density

From the analytical solution under low Reynolds numbers it is found that the migration velocities are independent of the ratios of density

Fig. 9. Effect of Reynolds numbers on migration velocity under different ratios of thermal conductivity.

and specific heat, while at high Reynolds numbers they will depend on the ratios of density and specific heat. In Fig. 10 the effect of Reynolds number on the migration velocities is shown under different ratios of density. The numerical results are consistent with the analytical solutions under low Reynolds numbers in that the density ratio has no effect on the migration velocities, while at high Reynolds numbers, the density ratio has slight effect on the migration velocity, especially for droplet. This is because at high Reynolds numbers the inertial effect becomes significant, with the decreasing density in continuous phase for droplet, the impedance of outer continuous phase is reduced, leading to high migration velocity.

3.4.4. Under different ratios of specific heat

In Fig. 11 the effect of Reynolds number on the migration velocities of droplet/bubble is shown under different ratios of specific heat, it is found that under low Reynolds numbers the specific heat ratio has no effect on the migration velocities because the viscous flow and heat conduction are dominant. At high Reynolds numbers the migration velocities are decreased dramatically because the inertial effect and convective heat transfer become dominant. It is noted that the ratio of specific heat has little effect on the migration velocity of droplet, while it has significant effect on the migration velocity of bubble. With the increasing ratio of specific heat the migration velocities of bubble are increased dramatically.

3.5. The effect of Reynolds number on Nusselt numbers

In order to examine the effect of Reynolds numbers on the temperature distributions in droplet/bubble with incoming thermal radiation, the Nusselt number is defined in Eq. (14d) based on the maximum temperature. If the heat transfer is stronger, the temperature distribution is more uniform with lower maximum temperature, thus the Nusselt number is higher.

3.5.1. Under different ratios of dynamic viscosity

In Fig. 12 the effect of Reynolds number on the Nusselt number is shown under different ratios of dynamic viscosity. It is expected that with the increasing Reynolds numbers all the Nusselt numbers increase, firstly mildly and then dramatically, it is because the convective heat transfer becomes dominant at high Reynolds numbers. Generally, the Nusselt number at higher ratio is lower, with the transition from bubble to droplet migration, the ratio of dynamic viscosity is decreased and the Nusselt number is increased slightly.

3.5.2. Under different ratios of thermal conductivity

Because the thermal conductivity has direct relationship with the heat transfer, it has more significant effect on the Nusselt number, as shown in Fig. 13. For both bubble and droplet migrations, the Nusselt numbers under low Reynolds number vary little and increase dramatically at high Reynolds numbers. It is interesting to note that at ratio $R_c = 1$, the Nusselt numbers are the highest. With the increasing ratio for bubble migration or decreasing ratio for droplet migration, the thermal conductivity in the gas region is decreased, the heat transfer is weakened, leading to high maximum temperature as well as low Nusselt number. It is also noted that at ratio $R_c = 10$ for bubble migration the Nusselt number is the lowest.

3.5.3. Under different ratios of density

In Fig. 14 the effect of Reynolds numbers on Nusselt number is shown under different density ratios. It is found that with the increasing Reynolds numbers the Nusselt numbers under different ratios of density all increase dramatically. At ratio $R_d = 1$ when the continuous phase has the same density with the discrete phase, the Nusselt numbers are the lowest, and at ratio $R_d = 10$ for the bubble migration the Nusselt numbers are the highest.

3.5.4. Under different ratios of specific heat

In Fig. 15 the effect of Reynolds numbers on the Nusselt numbers is shown under different ratios of specific heat. It is shown that at low Reynolds number the ratio has slight effect on the Nusselt numbers, while at high Reynolds number the ratio has dramatic effect. At ratio $R_{C_p} = 1$ the Nusselt numbers are the highest, with increasing ratio for bubble migration or decreasing ratio for droplet migration the Nusselt numbers are decreased, and they are the lowest at ratio $R_{C_p} = 10$ for bubble migration because the heat transfer is the weakest.

4. Conclusion

The spontaneous droplet/bubble migration due to thermal capillary force under uniform incoming thermal radiation is numerically simulated through the two-dimensional axisymmetric model with a level set method. The migration velocities and Nusselt numbers are provided under different ratios of dynamic viscosity, thermal conductivity, density and specific heat as well as different Reynolds numbers, the main findings are as follows:

1. The droplet/bubble can migrate spontaneously under thermal radiation due to thermal capillary effect, the driving force is from the positive pressure drop in the middle region of droplet/bubble.
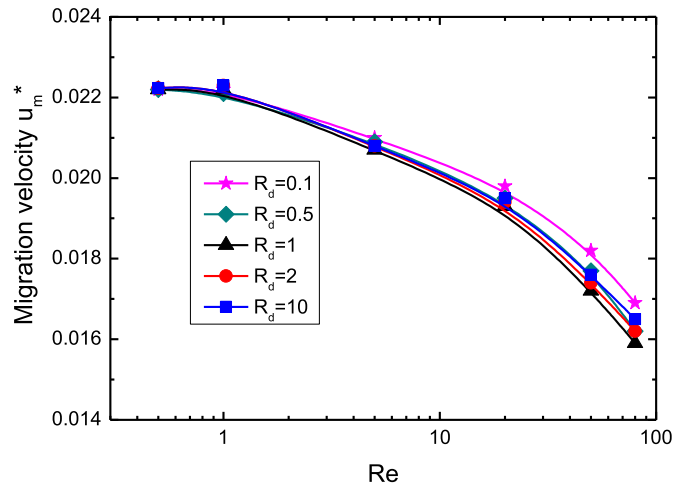

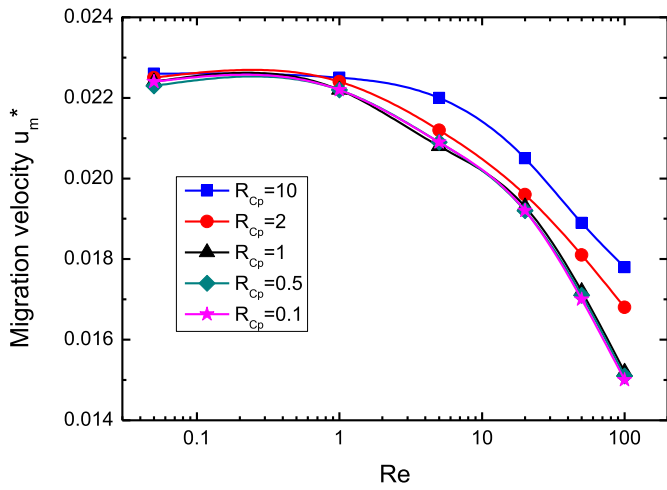**Fig. 10.** Effect of Reynolds numbers on migration velocity under different ratios of density.

Fig. 11. Effect of Reynolds numbers on migration velocity under different radio of specific heat.
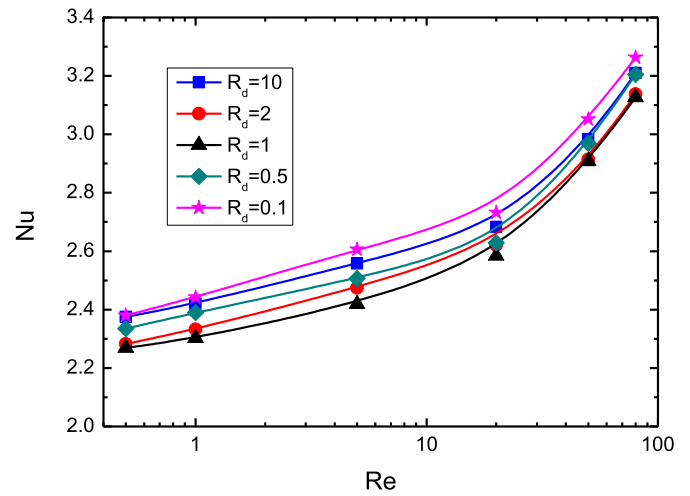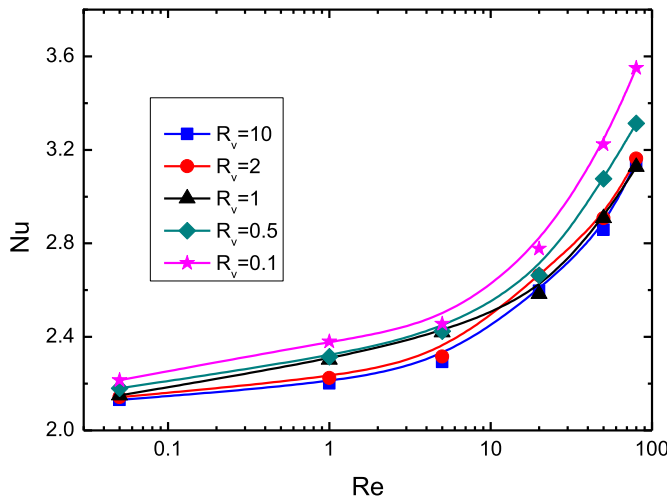

Fig. 12. Effect of Reynolds numbers on Nusselt numbers under different ratios of dynamic viscosity.

Fig. 13. Effect of Reynolds numbers on Nusselt numbers under different ratios of thermal conductivity.
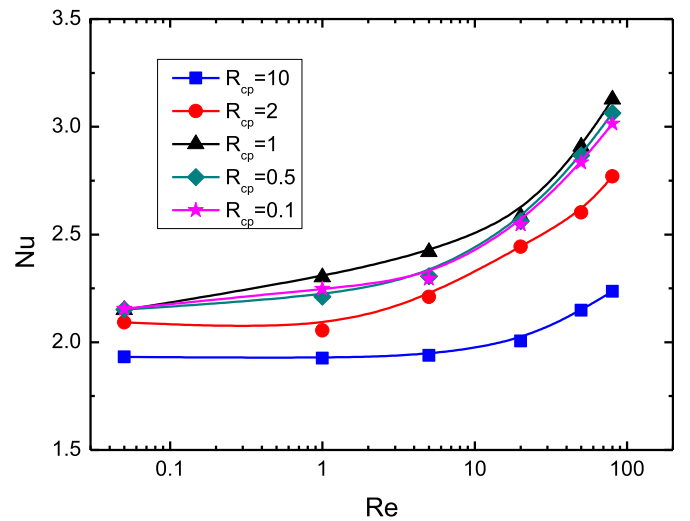

Fig. 14. Effect of Reynolds numbers on Nusselt numbers under different ratios of density.

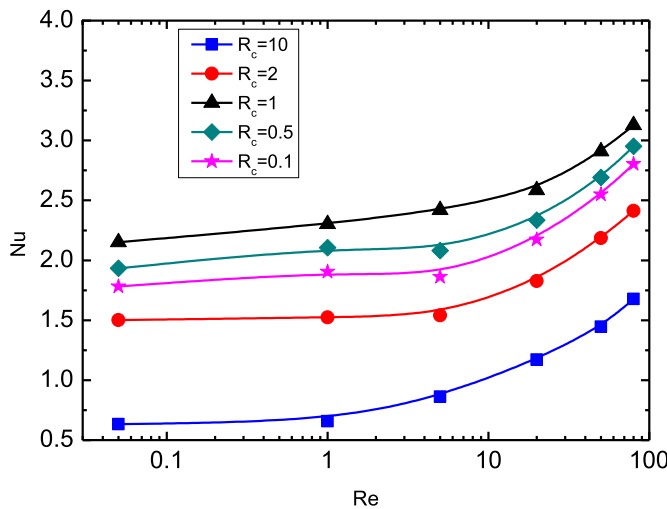**Fig. 15.** Effect of Reynolds numbers on Nusselt numbers under different ratios of specific heat.

2. Under low Reynolds numbers the migration velocities depend only on the ratios of dynamic viscosity and thermal conductivity, while under high Reynolds numbers the migration velocities also depend on ratios of density and specific heat.

3. When the dynamic viscosity or thermal conductivity in the continuous phase is equal to that in the discrete phase, the migration velocity is the minimum. With the increasing difference of dynamic viscosity or thermal conductivity between continuous phase and discrete phase, the migration velocity is increased.

4. The Nusselt numbers increase with the increasing Reynolds numbers. When the ratios of dynamic viscosity, thermal conductivity or specific heat are the largest for bubble migration, the Nusselt numbers are the lowest.

Acknowledgement

References

[1] R. Balasubramaniam, C.E. Lacy, G. Woniak, R.S. Subramanian, Thermocapillary migration of bubbles and drops at moderate values of the Marangoni number in reduced gravity, Phys Fluids 8 (4) (1996) 872–880.

[2] N.O. Young, J.S. Goldstein, M.J. Block, The motion of bubbles in a vertical temperature gradient, J Fluid Mech 6 (3) (2006) 350–356.

[3] R. Balasubramaniam, A.T. Chai, Thermocapillary migration of droplets: an exact solution for small marangoni numbers, J Colloid Interface Sci 119 (2) (1987) 531–538.

[4] A. Crespo, E. Migoya, F. Manuel, Thermocapillary migration of bubbles at large Reynolds numbers, Int J Multiphas Flow 24 (4) (1998) 685–692.

[5] A. Crespo, J. Jimenez-Fernandez, Thermocapillary migration of bubbles: a semi-analytical solution for large Marangoni numbers, 8th European symposium on materials and fluid sciences in microgravity, 1992, pp. 193–196.

[6] R.L. Thompson, K.J. Dewitt, T.L. Labus, Marangoni bubble motion phenomenon in zero gravity, Chem Eng Commun 5 (1980) 299–314.

[7] J.C. Xie, H. Lin, P. Zhang, F. Liu, W.R. Hu, Experimental investigation on thermocapillary drop migration at large Marangoni number in reduced gravity, J Colloid Interface Sci 285 (2) (2005) 737–743.

[8] J.A. Szymczyk, G. Wozniak, J. Siekmann, On Marangoni bubble motion at higher Reynolds- and Marangoni-numbers under microgravity, Appl Microgravity Technol 1 (1) (1987) 27–29.

[9] R. Balasubramaniam, J.E. Lavery, Numerical simulation of thermocapillary bubble migration under microgravity for large Reynolds and marangoni numbers, Numer Heat Tran A 16 (1989) 175–187.

[10] X.J. Ma, R. Balasubramaniam, R.S. Subramanian, Numerical simulation of thermocapillary drop motion with internal circulation, Numer Heat Tran A 35 (1999) 291–309.

[11] H. Haj-Hariri, Q. Shi, A. Borhan, Thermocapillary motion of deformable drops at finite Reynolds and Marangoni numbers, Phys Fluids 9 (4) (1997) 845–855.

[12] Z. Yin, P. Gao, W. Hu, L. Chang, Thermocapillary migration of nondeformable drops, Phys Fluids 20 (8) (2008) 350.

[13] Z. Yin, L. Chang, Q. Li, H. Wang, Numerical simulations on thermocapillary migrations of nondeformable droplets with large Marangoni numbers, Phys Fluids 24 (9) (2012) 356.

[14] Z.B. Wu, Terminal thermocapillary migration of a droplet at small Reynolds numbers and large Marangoni numbers, Acta Mech 228 (6) (2017) 2347–2361.

[15] D.L.R. Oliver, K.J. Dewitt, Surface tension driven flows for a droplet in a microgravity environment, Int J Heat Mass Tran 31 (1988) 1534–1537.

[16] B. Braun, C. Ikier, H. Klein, D. Woermann, Thermocapillary migration of droplets in a binary mixture with miscibility gap during liquid/liquid phase separation under reduced gravity, J Colloid Interface Sci 159 (2) (1993) 515–516.